Hydroxylation of Aromatics with Hydrogen Peroxide over Titanosilicates with MOR and MFI Structures: Effect of Ti Peroxo Species on the Diffusion and Hydroxylation Activity

Peng Wu, Takayuki Komatsu,* and Tatsuaki Yashima

Department of Chemistry, Tokyo Institute of Technology, 2-12-1 Ookayama, Meguro-ku, Tokyo 152-8551, Japan

Received: July 10, 1998

The shape selectivity in the liquid-phase hydroxylation of aromatic hydrocarbons with hydrogen peroxide has been studied on two kinds of titanosilicate, the large-pore Ti-M with MOR structure and medium-pore TS-1 with MFI structure, and the liquid-phase diffusion of aromatics into both catalysts was compared in the presence of H_2O and H_2O_2 to clarify the origin of the shape selectivity. The hydroxylation rate on TS-1 decreased monotonically with increasing molecular size in the order benzene > toluene ≫ ethylbenzene > cumene, while Ti−M showed the maximum rate for toluene hydroxylation. The apparent diffusivity of aromatics was lowered roughly by 1 order by adding H_2O_2 to H_2O solvent for both titanosilicates but was not affected for their Ti-free derivatives, mordenite and silicalite-1. The reduction in diffusion rate in the presence of H_2O_2 was more pronounced for TS-1 and for Ti-rich samples. It is concluded that a bulky Ti peroxo species (Ti−OOH) formed by the interaction of Ti site with H_2O_2 mainly causes a transition-state shape selectivity in the hydroxylation of bulky aromatics in titanosilicate/H_2O_2 systems.

Introduction

Titanium-containing silicalite molecular sieves have attracted great interest in zeolite chemistry and catalysis during the past decade. Extensive studies on the Ti-containing derivative of MFI-type zeolite (TS-1) have verified that it is an active catalyst for numerous oxidation reactions including phenol hydroxylation, alkane and alcohol oxidation, alkene epoxidation, and ketone ammoximation with aqueous hydrogen peroxide as an oxidant under mild conditions.[1−6] The successes in TS-1 investigations have promoted intensive research on this topic, which leads to the synthesis of medium-pore TS-2[7] and Ti−ZSM-48,[8] large-pore Ti-β[9] and TAPSO-5,[10] and more recently Ti-containing mesoporous materials, Ti−MCM-41[11] and Ti−MCM-48.[12] One of the secondary synthesis methods, that is, a treatment of highly siliceous zeolites with titanium chloride vapor at elevated temperatures, has also been adopted to prepare titanosilicates.[13] Especially using this method (named atom planting), we have succeeded in preparing large-pore titanium mordenite (Ti-M) which has not been hydrothermally synthesized yet.[14] Ti-M thus prepared showed higher activity than TS-1 in the hydroxylation of bulkier aromatics with H_2O_2[15] and was also an especially active and selective catalyst for the ammoximation of ketone to oxime.[16]

Various techniques have been adopted to understand the nature of Ti active sites in titanium silicalite. By means of XRD, IR, UV, Raman, XPS, EXAFS-XANES, and isotope exchange experiments,[17−28] the active sites of titanosilicate are believed to be those isolated Ti atoms located in the framework positions, while their coordination states may vary between 4- and 6-fold coordination depending on the dehydration or hydration.[23,24,29] In an actual oxidation reaction over TS-1 with H_2O_2, a framework Ti atom would react with a H_2O_2 molecule to from a Ti peroxo species (Ti−OOH) which would further interact with a donor hydroxyl to form a stable complex with five-membered cyclic structure.[28,30] The donor hydroxyl may be from an Si−OH group or a solvent molecule, such as H_2O and alcohols. This complex is proposed to be the real active site for TS-1 catalyzed reactions. The fact that the activity for the epoxidation of propylene became lower as the size of alcohol increased[31] would support the existence of this complex. Moreover, TS-1 is nearly inactive when the oxidation reactions are performed with a bulkier oxidant, *tert*-butyl hydroperoxide (TBHP), instead of H_2O_2,[32] owing to the difficulty of TBHP to diffuse into the pores and the blocking effect of larger Ti−OO−C$(CH_3)_3$ species. In the case of large-pore Ti-β, these steric effects were less pronounced.[33] These facts also verify indirectly the formation of Ti peroxo species. However, because the peroxo species is unstable to release H_2O_2 in the solvent, many attempts to obtain the pure Ti−OOH species have ended in failure until Clerici et al. succeeded for the first time in the preparation of peroxo species within TS-1 using a basic medium to increase its stability.[34]

From the viewpoint of shape selectivity, TS-1 used in the liquid-phase reactions seems to have a narrower pore size than its aluminosilicate derivative, ZSM-5, used in the gas-phase reactions. The former catalyzes with relatively high activity the oxidation or epoxidation of linear alkanes and alkenes and the hydroxylation of phenol and benzene, but it hardly catalyzes the reactions of cyclic alkanes, cyclic alkenes, and aromatics bulkier than benzene.[3] On the contrary, the latter catalyzes toluene or ethylbenzene alkylation, toluene disproportionation, xylene isomerization, and cumene cracking.[35−37] Though the reaction conditions are different for these cases, it must be an open question whether these differences between TS-1 and ZSM-5 are simply attributed to the reactant shape selectivity. Moreover, it could be possible that the Ti peroxo active species in the TS-1 catalyzed reactions affects the shape selectivity.

In this study, we have compared in detail the catalytic activity for the aromatic hydroxylation with the adsorption behavior

* To whom correspondence should be addressed. TEL +81-3-5734-2602; FAX +81-3-5734-2758; E-mail komatsu@chem.titech.ac.jp.

10.1021/jp982951t CCC: $15.00 © 1998 American Chemical Society
Published on Web 10/22/1998

using two kinds of titanosilicate having different pore sizes, TS-1 and Ti-M as catalysts and/or adsorbents, and aromatic hydrocarbons having different molecular sizes as reactants or adsorbates. The purpose of this study is to clarify the nature and origin of the shape selectivity of titanosilicate in the liquid-phase hydroxylation with H_2O_2. How the Ti peroxo species affects the shape selectivity of titanosilicate during the hydroxylation will be discussed based on the results of the liquid-phase adsorption of aromatics on TS-1 and Ti-M in the presence of H_2O_2.

Experimental Section

Materials. H-mordenite, M(8.2) (framework Si/Al atomic ratio of 8.2), was used for the dealumination. The dealumination procedure consisted of the calcination in air at 973 K followed by a reflux with 6 N HNO_3, as described previously in detail.[38] This procedure was repeated to obtain a highly siliceous mordenite, M(300). M(300) was then treated with $TiCl_4$ vapor (1.7 kPa) at 773 K for 5 min−2 h to prepare titanium mordenite, Ti-M(300). The details of this method (atom planting) were reported elsewhere.[14] MFI-type titanosilicates, TS-1(50), TS-1(70), and TS-1(104) (Si/Ti atomic ratios of 50, 70, and 104, respectively), were hydrothermally synthesized according to the patent using tetraethyl orthotitanate (TEOT) and tetraethyl orthosilicate (TEOS) as Ti and Si sources, respectively.[1] MFI-type silicalite (silicalite-1) was hydrothermally synthesized as reported previously.[39]

Hydroxylation of Aromatic Hydrocarbons. The hydroxylation of aromatic hydrocarbons with H_2O_2 was carried out in a 50 mL flask reactor at 363 K under vigorous agitation. The temperature of the flask was controlled with an oil bath. In a typical run, 50 mg of catalyst was stirred with 20 mL of aromatic substrate and 2 mL of H_2O. After the temperature of the mixture reached 363 K, the reaction was started by adding 1 mL of H_2O_2 (30 wt %). The products were analyzed periodically with a gas chromatograph (Shimadzu GC-14A) and quantified using *p*-ethylphenol or 2,6-xylenol as an external standard.

Liquid-Phase Adsorption and Characterization Methods. The liquid-phase adsorption was carried out in a glass cell with a capacity of 5 mL using 1,3,5-triisopropylbenzene (TIPB) as a solvent because it is believed to have a too large dimension (8.6 Å) to enter the pores of both MFI and MOR structures.[40,41] Because the catalyst was used for the hydroxylation without any dehydration pretreatment and the hydroxylation was carried out with water as a solvent, all samples were stored in water vapor over a saturated solution of NH_4Cl for at least 3 days before the adsorption experiments to make the influence of water similar to that during the hydroxylation. In a typical adsorption measurement, a known amount (0.1 g) of sample was mixed with 0.3 mL of H_2O or H_2O_2 (30 wt %) in the cell and agitated continuously with a stirrer to dissipate the heat evolved by the adsorption. The cell temperature was maintained at 273 K with an ice−water bath. The adsorption was started by injecting 2 mL of adsorbate solution (1 wt % of aromatic hydrocarbon in TIPB) into the cell. This amount of adsorbate was in large excess of adsorption capacity of the adsorbents. Therefore, the change in concentration of the adsorbate during the adsorption will not affect the rate of adsorption. A small portion of the liquid (about 0.1 μL) was taken periodically and analyzed with GC to determine the adsorption amount.

The Ti content was measured by inductively coupled plasma (ICP, Seiko SPS 1500VR) after the titanosilicate had been dissolved in an HF solution. Atomic absorption spectrophotometry (Shimadzu AA-640-12) was used to measure Al content.

TABLE 1: Physicochemical Properties of Various Catalysts

sample	Ti content/ mmol g^{-1}	Al content/ mmol g^{-1}	cryst size/μm	specific surf. area/ m^2 g^{-1}	amt of N_2 adsorpn/ mL g^{-1}
M(8.2)	0	1.65	1	557	0.18
M(300)	0	0.020	1	588	0.19
Ti-M(300)[a]	0.142	0.018	1	553	0.18
silicalite-1	0	0	6	499	0.16
TS-1(104)	0.151	0	0.2	564	0.18
TS-1(70)	0.228	0	0.2	549	0.17
TS-1(50)	0.314	0	0.2	582	0.17

[a] Ti-M(300) was prepared by the treatment of M(300) with $TiCl_4$ vapor (1.7 kPa) at 773 K for 1 h.

Surface area was measured by N_2 adsorption at 77 K (Coulter SA 3100). IR spectra were recorded on a Shimadzu FTIR-8100 spectrometer at room temperature after the sample pressed into a self-supporting wafer with 4.8 mg cm^{-2} thickness was evacuated in a quartz IR cell at 473 K for 1 h. Scanning electron micrographs (SEM, JEOL JSM-T220) were recorded to determine crystal sizes.

Results and Discussion

Material Characterizations. Table 1 shows the physicochemical properties of various catalysts used in this study. Through the dealumination treatment on a hydrothermally synthesized mordenite, M(8.2), a highly siliceous mordenite, M(300), containing only trace amount of Al was obtained. The further treatment of M(300) with $TiCl_4$ vapor at 773 K for 1 h resulted in titanium mordenite, Ti-M(300). IR, UV, and isotope-exchange experiments[14−16] have confirmed that almost all the Ti atoms in Ti-M(300) are tetrahedrally located in the framework sites as well as those in hydrothermally synthesized TS-1. No obvious collapse in the crystalline structure was detected by XRD for these samples, and their specific surface area and the amount of N_2 adsorption as shown in Table 1 were comparable to those reported in the literature. The morphology of mordenite crystals was mainly pillar-shaped with a few flat and prismatic crystals, and their average size was ca. 1 μm (Figure 1a,b). The crystals of silicalite-1 were slightly elongated euhedral with a length of ca. 6 μm (c), just as reported previously.[39] TS-1(104) showed a typical cubic morphology and had a uniform crystal size of ca. 0.2 μm (d). The morphology and crystal size did not change significantly with the Si/Ti atomic ratios for three TS-1 samples. It is clear that the samples used in the present study except for silicalite-1 consist of very small crystals. Accordingly, we neglected the influence of diffusion through channels having largely different length, that is, the external fluid side mass transfer resistance in the liquid-phase adsorption.[42,43] No amorphous phases were observed in the scanning electron micrographs of all samples with both MOR and MFI structures. Together with N_2 adsorption experiments, it is clear that all the samples used in the present study were highly crystalline materials.

Hydroxylation of Aromatics over Ti-M and TS-1. We have previously compared between the hydroxylation activity of Ti-M and TS-1 for monoalkyl aromatics and xylene isomers at a definite reaction time of 2 h and found that Ti-M is more active than TS-1 in the hydroxylation of bulkier aromatics.[15] To further compare their shape selectivity and to clarify the relationship between the hydroxylation activity and the diffusion rate, the kinetic time processes of the hydroxylation of aromatics with various molecular sizes have been carried out on Ti-M(300) and TS-1(104) which had comparable Ti content (Figure 2). The oxidation of side alkyl groups to form alcohols, aldehydes,

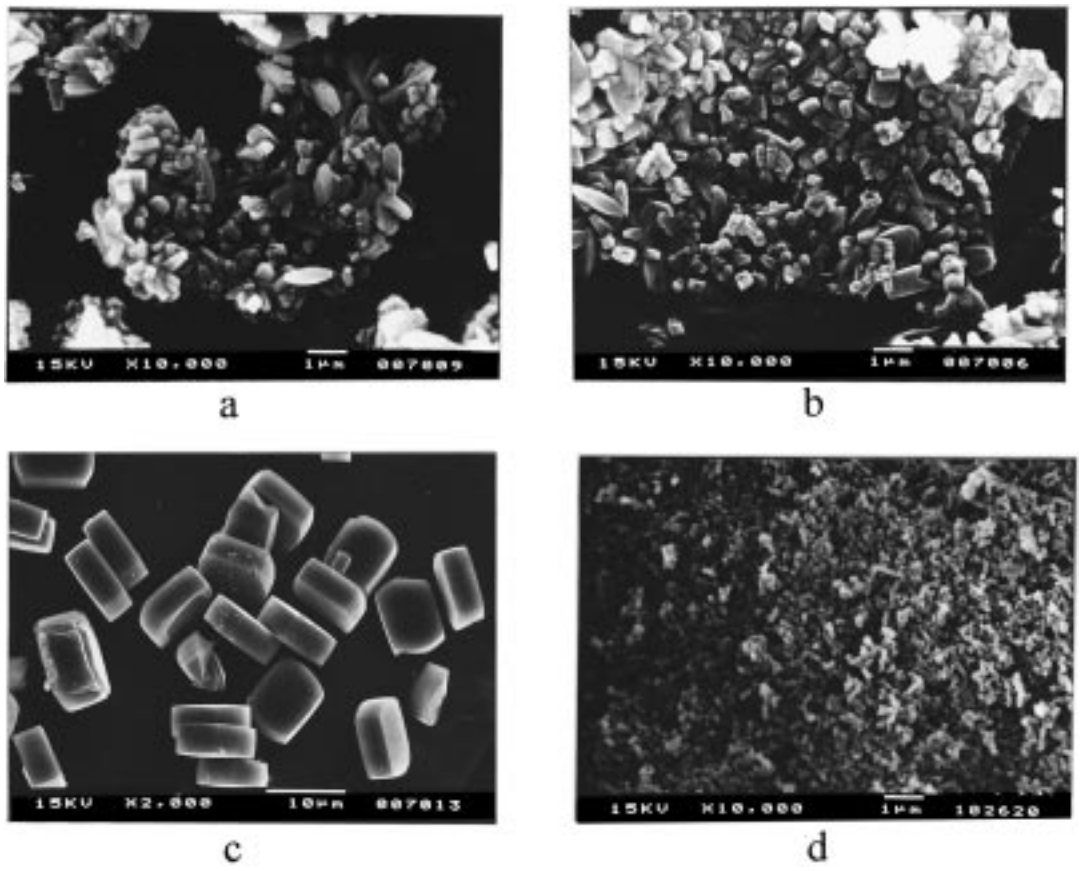

Figure 1. Scanning electron micrographs of M(8.2) (a), Ti-M(300) (b), silicalite-1 (c), and TS-1(104) (d).

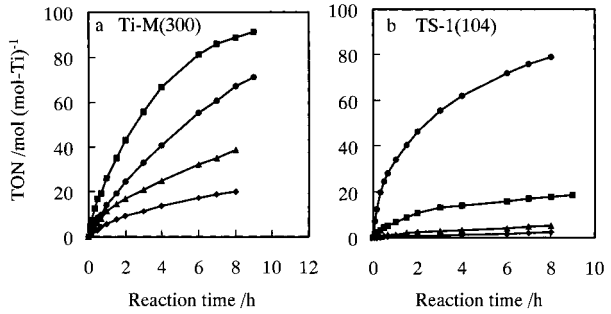

Figure 2. Hydroxylation of benzene (●), toluene (■), ethylbenzene (▲), and cumene (◆) on Ti-M(300) (a) and TS-1(104) (b). Conditions: catalyst, 50 mg; temperature, 363 K; substrate, 20 mL; H_2O, 2 mL; H_2O_2 (30 wt %), 1 mL.

and ketones occurred even in the noncatalyzed reactions, but their selectivity in the catalytic runs was lower than 1%. The substitution of side alkyl groups by the hydroxyl group to form phenol hardly occurred for toluene and ethylbenzene but occurred for cumene. The reaction in which a hydroxyl group substitutes an isopropyl group of cumene to form a phenol molecule may proceed through an intermediate of cumene hydroperoxide just like a commercial process for phenol production. This reaction does not certainly occur within the zeolite channels. For these reasons, only the yield of products through the benzene ring hydroxylation, which must be catalyzed by the Ti species inside the zeolite pores, was used to evaluate the activity of Ti-M and TS-1.

The activity was expressed as turnover number (TON) per Ti site. As shown in Figure 2a, Ti-M catalyzed the hydroxylation of four aromatic substrates readily although the TON varied among the substrates. The order of reaction rate on the Ti-M catalyst was toluene > benzene > ethylbenzene > cumene. Benzene ring hydroxylation is thought to be an electrophilic attack by Ti species. Consequently, the reactivity of substrates would increase when electron-donating alkyl groups attach to the benzene ring. The strength of this activation for benzene ring is in the order of $-CH(CH_3)_3 > -CH_2CH_3 > -CH_3$. This would explain why the reaction rate observed for toluene was higher than that for benzene. However, this was not the case for ethylbenzene and cumene as Ti-M showed lower TON for them. For ethylbenzene and cumene, steric hindrance and/or diffusion limitation may dominate the reaction rates to lower their TON.

On the other hand, the order of TON for the TS-1(104) catalyst was benzene > toluene ≫ ethylbenzene > cumene (b). The initial reaction rate of benzene hydroxylation on medium-pore TS-1 was even higher than that on large-pore Ti-M, which may be because the residual Al remaining in Ti-M lowers the intrinsic activity of Ti sites by altering the electron density around them.[15,44] In contrast with the results on Ti-M, the $-CH_3$ group attaching to the benzene ring did not enhance but reduced the hydroxylation rate, and the bulkier alkyl groups, $-CH_2-CH_3$ and $-CH(CH_3)_2$, made TS-1 almost inactive for the hydroxylation. These results suggest that the hydroxylation of aromatics over TS-1 is kinetically dominated by the diffusivity of substrates. The obvious difference between Ti-M and TS-1 in the hydroxylation of various aromatics seems to be due to the shape selectivity owing to their different pore sizes. However, it is not quite reasonable that the very lower activity of TS-1 for the hydroxylation of ethylbenzene and cumene is simply attributed to its reactant shape selectivity because its aluminosilicate derivative, ZSM-5, catalyzes readily ethylbenzene alkylation and cumene cracking in solid−gas reactions though the reaction temperatures are higher.[36,37] To clarify the diffusion effects on the hydroxylation, we have carried out the

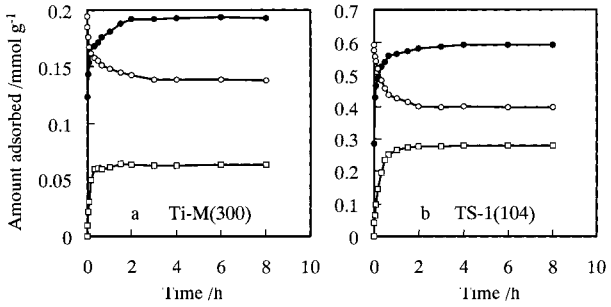

Figure 3. Adsorption uptake curves of *m*-cresol (●), toluene (□) after *m*-cresol adsorption, and *m*-cresol (○) during the toluene adsorption on Ti-M(300) (a) and TS-1(104) (b). Adsorption conditions: catalyst, 0.1 g; temperature, 273 K; H_2O, 0.3 mL; adsorbate (1 wt % in TIPB), 2 mL. The adsorption of *m*-cresol alone was first carried out, and subsequently the adsorption of toluene was carried out on *m*-cresol-saturated samples.

adsorption experiments in the liquid phase under the conditions similar as possible to those adopted for the hydroxylation reactions.

Effect of Product on the Diffusion of Reactant in the Liquid Phase. Since the alkylphenol products formed from the ring hydroxylation are larger than the aromatic reactants, they would hinder the diffusion of reactants once they are formed within the zeolite channels. Therefore, we have compared the effect of product on the diffusion of reactant in Ti-M with that in TS-1 using toluene as a reactant. On both Ti-M and TS-1, toluene was converted into three cresol isomers. Among them, *m*-cresol was used to investigate its influence on the diffusion of toluene because *m*-cresol has the largest molecular size. Figure 3 shows the adsorption uptake curves for Ti-M(300) and TS-1(104). It should be noted that any difference in the adsorption capacity from that reported in the literatures is hardly due to the low crystallinity of the present samples because Table 1 and Figure 1 have verified their high crystallinity. Since the adsorbents were not subjected to any pretreatment to make the conditions similar to those used in the liquid-phase hydroxylation, the adsorption would occur through the ejection of preadsorbed water molecules out of the zeolite channels. As shown by solid symbols, *m*-cresol diffused into the channels of both Ti-M and TS-1, and the adsorption amount was saturated within 2 h. The adsorption capacity of *m*-cresol on TS-1 was about 3 times that on Ti-M, which would result from the higher hydrophilicity of Ti-M containing residual Al. After the adsorption of *m*-cresol reached the equilibrium in 8 h, a certain amount of toluene solution was added into the system to see how preadsorbed *m*-cresol influenced the diffusion of toluene into the zeolite channels. Toluene molecules diffused into the channels of both Ti-M and TS-1 saturated with *m*-cresol to reach the equilibrium rapidly, while the preadsorbed *m*-cresol was partially driven out of the channels as indicated by the decrease in its adsorption amount. No obvious difference in the effect of *m*-cresol on the toluene diffusion has been observed between Ti-M and TS-1. Therefore, the difference in the activity of Ti-M and TS-1 for toluene hydroxylation shown in Figure 2 is hardly explained by the retardation effect of bulky products, cresol isomers, on the diffusion of reactant.

Diffusion of Aromatics in the Presence of H_2O and H_2O_2. As the active sites in TS-1 for the reactions with hydrogen peroxide has been reported to be Ti peroxo complex,[28,30] this species may affect the above shape selectivity observed in the hydroxylation of aromatics over Ti-M and TS-1. To confirm this issue, the liquid-phase adsorption of various aromatics on Ti-M and TS-1 has been carried out in the presence of H_2O

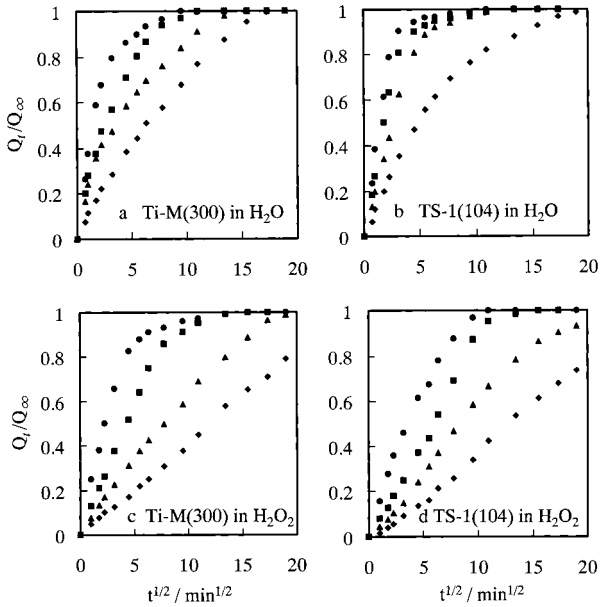

Figure 4. Relative adsorption uptake of benzene (●), toluene (■), ethylbenzene (▲), and cumene (◆) in H_2O (a, b) and H_2O_2 (c, d) on Ti-M(300) (a, c) and TS-1(104) (b, d). Adsorption conditions: catalyst, 0.1 g; temperature, 273 K; H_2O or H_2O_2 (30 wt %), 0.3 mL; adsorbate (1 wt % in TIPB), 2 mL.

and H_2O_2. The adsorption temperature of 273 K was chosen to suppress the hydroxylation of benzene ring during the adsorption process in the presence of H_2O_2. Figure 4 shows the dependence of the relative adsorption uptake on square root of time, where Q_t and Q_∞ denote the mass adsorbed at time t and infinite time, respectively. The Q_∞ value was taken from the saturated amount in each uptake curve.

The diffusion rates of various aromatics followed the order of their molecular size as expected, that is, benzene > toluene > ethylbenzene > cumene, for both Ti-M and TS-1 independent of the presence of H_2O_2. In the presence of H_2O, the adsorption of the largest molecule, cumene, reached the equilibrium within 7 h for Ti-M (a) and even for TS-1 (b). However, the diffusion rate was reduced greatly by replacing H_2O with H_2O_2. As shown in Figure 4c,d, the time required to reach the equilibrium adsorption was prolonged for all the adsorbates on Ti-M and TS-1. The linear relationship found for the uptake curves in the initial region suggests that the kinetics of adsorption is mainly governed by intracrystalline diffusion within the microparticles. Therefore, assuming that the adsorbent particles are spherical, we refer the slopes in the initial region to a simplified equation for the evaluation of apparent diffusivity, D/r^2, and diffusivity, D:[45]

$$\frac{Q_t}{Q_\infty} = \frac{6}{\pi^{1/2}}\left(\frac{D}{r^2}\right)^{1/2} t^{1/2} \qquad (1)$$

while r denotes the average radius of adsorbent particle. D/r^2 obtained according to eq 1 from the slopes of the uptake curves in the initial region are compared in Table 2. It is obvious that the replacement of H_2O with H_2O_2 reduced the D/r^2 value roughly by 1 order for each adsorbate on both Ti-M and TS-1. For a better understanding of the effects of solvents on the diffusivity, we have compared the relative diffusivity of each adsorbate to that of the smallest molecule, benzene, as shown in Figure 5. The relative diffusivity decreased from benzene to cumene for both Ti-M and TS-1 independent of the solvents. The higher relative diffusivity of Ti-M than that of TS-1 for

TABLE 2: Apparent Diffusivity, D/r^2 (10^{-5} s^{-1}), of Various Adsorbates in the Presence of H_2O and H_2O_2[a]

	Ti-M(300)		TS-1(104)		M(300)		silicalite-1	
adsorbate	in H_2O	in H_2O_2	in H_2O	in H_2O_2	in H_2O	in H_2O_2	in H_2O	in H_2O_2
benzene	16.5	8.4	20.1	4.1				
toluene	12.7	2.2	13.1	0.9	12.7	12.4	18.9	18.3
ethylbenzene	7.3	0.9	6.5	0.3				
cumene	1.5	0.3	2.0	0.1				

[a] Adsorption conditions, see Figure 4.

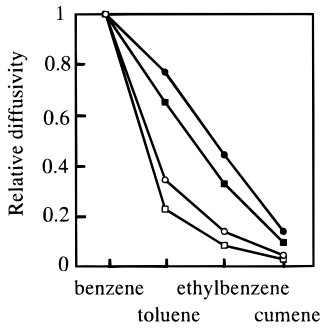

Figure 5. Relative diffusivity of aromatics having different molecular sizes for Ti-M(300) with water (●) or H_2O_2 (○) and TS-1(104) with water (■) or H_2O_2 (□). The relative diffusivity was obtained as the diffusivity of benzene on the same adsorbent to be unity.

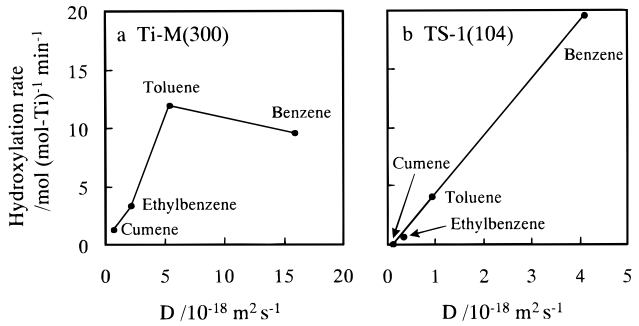

Figure 6. Dependence of hydroxylation rate on diffusivity of aromatics in Ti-M(300) (a) and TS-1(104) (b) in the presence of H_2O_2.

bulkier adsorbates would be attributed to their difference in channel size. The lower relative diffusivity in H_2O_2 than that in H_2O for both Ti-M and TS-1 strongly implies that the Ti peroxo species has an important influence on the diffusion of adsorbates. The hydroxylation behavior shown in Figure 2 may be governed by the transition-state shape selectivity because the transition state of reacting molecule must be formed on the Ti peroxo active site where steric hindrance will be severest in the pore. To confirm this hypothesis, the liquid-phase adsorption of toluene in the presence of H_2O and H_2O_2 was also carried out on Ti-free M(300) and silicalite-1. As shown in Table 2, the apparent diffusivity (D/r^2) in H_2O_2 did not decrease significantly from that in H_2O in the case of both Ti-M and silicalite-1. It is concluded that H_2O_2 retards the diffusion of aromatics only when the silicalite framework contains Ti atoms. A bulky species should be formed through the reaction between Ti and H_2O_2.

Figure 6 shows the dependence of the hydroxylation rate on the diffusivity (D) for various aromatics in the presence of H_2O_2. The hydroxylation rate on Ti-M increased with increasing D for cumene, ethylbenzene, and toluene but decreased slightly with further increasing D for benzene (a). It is deduced that the diffusion of substrate within the channels is the rate-controlling step in the hydroxylation of the former aromatics,

TABLE 3: Adsorption Capacity, Q_∞ (mmol g^{-1}), of Various Adsorbates in the Presence of H_2O and H_2O_2[a]

	Ti-M(300)		TS-1(104)		M(300)		silicalite-1	
adsorbate	in H_2O	in H_2O_2	in H_2O	in H_2O_2	in H_2O	in H_2O_2	in H_2O	in H_2O_2
benzene	0.65	0.45	0.79	0.77				
toluene	0.43	0.32	0.67	0.64	0.46	0.45	0.75	0.78
ethylbenzene	0.31	0.29	0.66	0.61				
cumene	0.25	0.21	0.51	0.49				

[a] Adsorption conditions, see Figure 4.

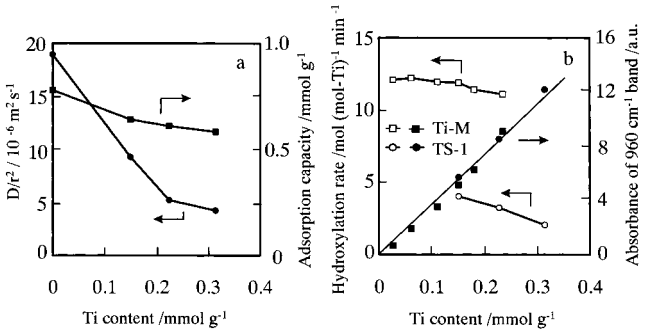

Figure 7. Dependence of D/r^2 and adsorption capacity of toluene on Ti content in TS-1 and silicalite-1 (a). Dependence of toluene hydroxylation rate and absorbance of 960 cm^{-1} IR band on Ti content in Ti-M and TS-1 (b). Toluene hydroxylation conditions are the same as in Figure 2.

while the activation of benzene ring by Ti peroxo species is the rate-determining step for the hydroxylation of benzene because the large pores of mordenite will accommodate benzene molecules easily even in the presence of Ti peroxo species. On the other hand, the hydroxylation rate on TS-1 increased almost linearly with the increase in D values, indicating the hydroxylation on medium-pore TS-1 is predominately controlled by the diffusion of substrate within the channels containing Ti peroxo species.

Effect of Ti Content on Diffusion and Hydroxylation. Generally, the adsorption capacity of zeolite and the diffusivity of an adsorbate are mainly determined by the size and shape of adsorbate molecule and zeolite pore. The replacement of H_2O with H_2O_2 in the liquid-phase adsorption not only hindered the diffusivity of adsorbate molecules within the channels but also slightly reduced the adsorption capacity, Q_∞ (Table 3), while the decrease in Q_∞ was not obvious on M(300) and silicalite-1. Therefore, Ti peroxo species formed in the titanosilicate/H_2O_2 system may occupy a certain volume within the channels. The density of Ti peroxo species is expected to play an important role in the adsorption, diffusion, and subsequently the reactivity of adsorbate in the titanosilicate/H_2O_2 system. To clarify this issue, the liquid-phase adsorption of toluene was carried out on TS-1 samples with different Ti contents. As shown in Figure 7a, the D/r^2 value decreased dramatically with increasing Ti content from Ti-free silicalite-1 to TS-1(104) and further decreased with increasing Ti content to TS-1(50). Simultaneously, the adsorption capacity of toluene also decreased gradually with increasing Ti content. Since Figure 6b verified that the hydroxylation rate of aromatics over TS-1 was mainly governed by the diffusion rate, the hydroxylation rate of toluene over TS-1 decreased reasonably with increasing Ti content (Figure 7b). For Ti-M, a series of samples with various Ti contents were prepared by treating M(300) with $TiCl_4$ vapor at 773 K for a different period and were also adopted to the hydroxylation of toluene. The hydroxylation rate was almost constant below 0.15 mmol g^{-1} Ti content and showed a slight

decrease over 0.15 mmol g^{-1}. In the similar Ti content region, Ti-M showed less decrease in hydroxylation rate than TS-1 with increasing Ti content, which is probably due to the larger pores of the former. It should be noted that this decrease in hydroxylation rate cannot be attributed to the presence of extraframework Ti species because all the Ti-containing zeolites used in the present study showed the characteristic IR band at 960 cm^{-1} due to tetrahedral Ti species,[14,15] and its intensity was proportional to the Ti content as shown in Figure 7b. Moreover, they exhibited only an absorption band at 220 nm in their UV−visible spectra, indicating the presence of tetrahedral Ti species.[15]

The formation of metal peroxo compounds through the reaction of metal oxides or metal complexes with either organic hydroperoxides or hydrogen peroxide is well-known for transition metals in groups 4−6. The change in color of titanosilicate from white into bright yellow immediately upon contact with H_2O_2 suggests the formation of Ti peroxo species, Ti−OOH. Bellussi et al.[28] proposed for TS-1 that the Ti−OOH species thus produced has a stable five-membered cyclic structure, with a donor hydroxyl moiety coordinated to Ti. The donor hydroxyl group may be provided by a solvent molecule or by a neighboring Si−OH group formed by cleaving Si−O−Ti bond with water. The solvent effect, that is, a decrease in the catalytic activity with bulkier alcohol, strongly suggests the coordination of hydroxyl group from the solvent to Ti site. Although many attempts to obtain the pure Ti peroxo species have ended in failure, the presence of the Ti peroxo species has also been verified by comparing the catalytic performance with H_2O_2 to that with *tert*-butyl hydroperoxide (TBHP). TS-1 was ineffective with TBHP even for the oxidation of reactants having no diffusion problem, while large-pore Ti-β was still effective with TIPB though the reaction proceeded at a lower rate and showed a higher transition-state selectivity than when using H_2O_2.[33] This was attributed to a higher steric constraint for the transition state of Ti−OOR species (R = $-C(CH_3)_3$) as compared with Ti−OOH. The only report for the preparation of Ti peroxo species for TS-1 was given by Clerici, who used a basic medium to enhance its stability.[34]

Here, we used an adsorption measurement for the first time to confirm the formation of Ti peroxo species in Ti-M or TS-1/H_2O_2 systems. A slight decrease in adsorption capacity (Table 3) and a dramatic decrease in diffusivity value (Table 2) when H_2O was replaced with H_2O_2 suggest that Ti peroxo species might be a bulky complex, like the five-membered cyclic structure hypothesized previously.[28] The species with hydrogen-bonded structure involving a Ti−OOH and a solvent molecule, H_2O, formed within zeolite channels is graphically described in Figure 8 for both Ti-M and TS-1. The diffusion problem and transition-state shape selectivity by the formation of this species would be more pronounced in the medium pore (5.4 × 5.6 A) of MFI than in the large pore (6.7 × 7.0 A) of MOR. This kind of shape selectivity would be stressed when several species gather in the neighborhood to further narrow the effective pore size of channels. As a special case, Figure 8 shows two Ti peroxo species occupying the same pore window.

Conclusions

The diffusion of aromatic hydrocarbons in the channels of titanosilicate with MOR and MFI structure is greatly affected by H_2O_2; it decreases by about 1 order when H_2O_2 is added to the adsorption system containing water. The higher the content of Ti in titanosilicate is, the lower the diffusion of aromatics. These results manifest the formation of bulky Ti peroxo species probably with five-membered cyclic structure within their channels. The shape selectivity more pronounced for TS-1 than for Ti-M in the hydroxylation of aromatics is mainly attributed to the strong steric constraint for the transition state to be formed within the medium-pore channels of MFI as compared to the large-pore channels of MOR.

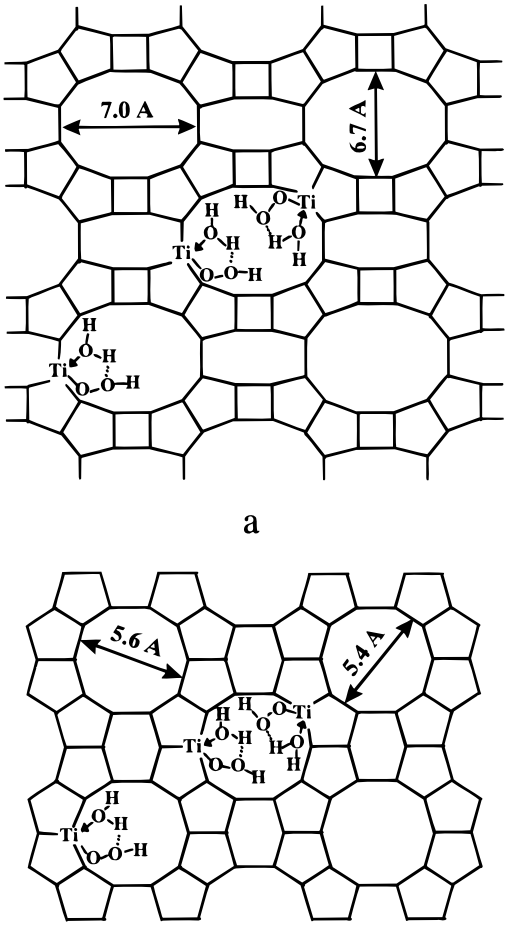

Figure 8. Proposed Ti peroxo species within the pores of Ti-M (a) and TS-1 (b).

References and Notes

(1) Tramasso, M.; Perego, G.; Notari, B. U.S. Patent 4,410,501, 1983.
(2) Perego, G.; Bellussi, G.; Corno, C.; Taramasso, M.; Buonomo, F.; Esposito, A. *Stud. Surf. Sci. Catal.* **1986**, *28*, 129.
(3) Bellussi, G.; Rigutto, M. S. *Stud. Surf. Sci. Catal.* **1994**, *85*, 177.
(4) Notari, B. *Stud. Surf. Sci. Catal.* **1988**, *37*, 413.
(5) Notari, B. *Catal. Today* **1993**, *18*, 163.
(6) Notari, B. *Adv. Catal*. **1996**, *41*, 253.
(7) Reddy, J. S.; Kumar, R.; Ratnasamy, P. *Appl. Catal.* **1990**, *58*, L1.
(8) Serrano, D. P.; Li, H.-X.; Davis, M. E. *J. Chem. Soc., Chem. Commun.* **1992**, 745.
(9) Camblor, M. A.; Corma, A.; Martínez, A.; Pérez-Pariente, J. *J. Chem. Soc., Chem. Commun.* **1992**, 589.
(10) Tuel, A. *Zeolites* **1995**, *15*, 228.
(11) Blasco, T.; Corma, A.; Navarro, M. T.; Pérez-Pariente, J. *J. Catal.* **1995**, *156*, 65.
(12) Koyano, A.; Tatsumi, T. *Stud. Surf. Sci. Catal.* **1997**, *105*, 93.
(13) Kraushaar, B.; van Hooff, J. H. C. *Catal. Lett.* **1988**, *1*, 81.
(14) Wu, P.; Komatsu, T.; Yashima, T. *J. Phys. Chem*. **1996**, *100*, 10316.
(15) Wu, P.; Komatsu, T.; Yashima, T. *Stud. Surf. Sci. Catal.* **1997**, *105*, 663.
(16) Wu, P.; Komatsu, T.; Yashima, T. *J. Catal*. **1997**, *168*, 400.
(17) Boccuti, M. R.; Rao, K. M.; Zecchina, A.; Leofanti, G.; Petrini, G. *Stud. Surf. Sci. Catal*. **1988**, *48*, 133.

(18) Huybrechts, D. R. C.; Buskens, P. L.; Jacobs, P. A. *J. Mol. Catal*. **1992**, *71*, 129.
(19) Khouw, C. B.; Dartt, C. B.; Labinger, J. A.; Davis, M. E. *J. Catal.* **1994**, *149*, 195.
(20) Khouw, C. B.; Davis, M. E. *J. Catal.* **1995**, *151*, 77.
(21) Behrens, P.; Felsche, J.; Vetter, F.; Schulz-Elkoff. G.; Jaeger, N. I.; Niemann, W. *J. Chem. Soc., Chem. Commun.* **1991**, 678.
(22) Lopez, A.; Kessler, H.; Guth, J. L.; Tuilier, M. H.; Popa, J. M. In *Proceedings of the 6th International Conference on X-ray Absorption Fine Structure, York, U. K., 1990*; Elsevier: Amsterdam, 1990; p 548.
(23) Trong On, D.; Bonneviot, L.; Bittar, A.; Sayari, A.; Kaliaguine, S. *J. Mol. Catal.* **1992**, *74*, 233.
(24) Bonneviot, L.; Trong On, D.; Lopez, A. *J. Chem. Soc., Chem. Commun.* **1993**, 685.
(25) Pei, S.; Zajac, G. W.; Kaduk, J. A.; Faber, J.; Boyanov, B. I.; Duck, D.; Fazzini, D.; Morrison, T. I.; Yang, D. S. *Catal. Lett.* **1993**, *21*, 333.
(26) Zecchina, A.; Spoto, G.; Bordiga, S.; Ferrero, A.; Petrini, G.; Leofanti, G.; Padovan, M. *Stud. Surf. Sci. Catal.* **1991**, *69*, 251.
(27) Tuel, A.; Taarit, Y. B. *Appl. Catal.* **1993**, *A102*, 69.
(28) Bellussi, G.; Carati, A.; Clerici, M. G.; Maddinelli, G.; Millini, R. *J. Catal.* **1992**, *133*, 220.
(29) Camblor, M. A.; Corma, A.; Pérez-Pariente, J. *J. Chem. Soc., Chem. Commun.* **1993**, 1557.
(30) Clerici, M. G.; Ingallina, P. *J. Catal.* **1993**, *140*, 71.
(31) Clerici, M. G.; Bellussi, G.; Romano, U. *J. Catal.* **1991**, *129*, 1.
(32) Romano, V.; Rsposito, A.; Maspero, F.; Neri, C.; Clerici, M. G. In *New Development in Selective Oxidation*; Centi, G., Trifiró, F., Eds.; Elesevier: Amsterdam, 1990; p 33.
(33) Corma, A.; Esteve, P.; Martínez, A.; Valencia, S. *J. Catal.* **1995**, *152*, 18.
(34) Clerici, M. G.; Ingallina, P.; Millini, R. In *Proceedings of the 9th International Zeolite Conference*; von Ballmoos, R., et al., Eds.; Butterworth-Heinemann: Woburn, MA, 1993; p 445.
(35) Kaeding, W. W.; Chu, C.; Young, L. B.; Butter, S. A. *J. Catal.* **1981**, *69*, 392.
(36) Kim, J.-H.; Namba, S.; Yashima, T. *Zeolites* **1991**, *11*, 59.
(37) Yamagishi, K.; Namba, S.; Yashima, T. *J. Catal.* 1**990**, *121*, 47.
(38) Wu, P.; Komatsu, T.; Yashima, T. *J. Phys. Chem*. **1995**, *99*, 10923.
(39) Yamagishi, K.; Namba, S.; Yashima, T. *J. Phys. Chem.* 1**991**, *95*, 872.
(40) Namba, S.; Kanai, Y.; Shoji, H.; Yashima, T. *Zeolites* **1984**, *4*, 77.
(41) Namba, S.; Yoshimura, A.; Yashima, T. *Chem. Lett*. **1979**, 759.
(42) (a) Ma, Y. H.; Lin, Y. S. *AIChE Symp. Ser*. **1983**, *83* (259), 1.
(43) Choudhary, V. R.; Singh, A. P. *Zeolites* **1986**, *6*, 206.
(44) Corma, A.; Camblor, M. A.; Esteve, P.; Martínez, A.; Pérez-Pariente, J. *J. Catal.* **1994**, *145*, 151.
(45) Kärger, J.; Ruthven, D. M. *Diffusion in Zeolites*; John Wiley & Sons: New York, 1992; p 230.